Control-based Design of a DELTA robot

Minglei Zhu, Abdelhamid Chriette, Sébastien Briot

Control-based Design of a DELTA Robot

Minglei Zhu[1,2], Abdelhamid Chriette[1,2], and Sébastien Briot[1,3]

[1] Laboratoire des Sciences du Numérique de Nantes (LS2N)
UMR CNRS 6004, 44321 Nantes, France
[2] École Centrale de Nantes
[3] Centre National de la Recherche Scientifique (CNRS)
{Minglei.Zhu,Abdelhamid.Chriette,Sebastien.Briot}@ls2n.fr

Abstract. In the present paper, a control-based design methodology is developed in order to create a DELTA robot with the best accuracy performance for a dedicated controller. The proposed control-based design methodology takes into account the accuracy performance of the controller in the design process to get the optimal geometric parameters of the robot. Three types of controllers are envisaged for the control of the motions of the DELTA robot: leg-direction-based visual servoing, line-based visual servoing and image moment visual servoing. Based on these three controllers, positioning error models taking into account the error of observation coming from the camera are developed. Then, design optimization problems are formulated in order to find the optimal geometric parameters and camera placement for the DELTA robot for each type of controller. Co-simulations of the robots optimized for the three types of controllers are finally performed in order to check the accuracy performance of the three robots.

1 Introduction

Parallel robots have several advantages with respect to serial robots, such as they can reach high speed and acceleration, better payload, are stiffer [1]. Nevertheless, compared to serial robots, the control of parallel robots is more difficult since such robots have a more complex structure and their input/output relations are highly non-linear.

Many research works focused on the control of parallel robots (see [2] for a long list of references). In general, in order to get high accuracy with a parallel robot, detailed models are necessary. However, even detailed models still suffer from the problem of inaccuracy in reality because of robot assembly and manufacturing errors. To bypass the complex kinematic architecture and to get a better accuracy compared to model-based controllers, an efficient method is the application of sensor-based controller which uses external sensors to estimate the pose of the end-effector [3]. Visual servoing uses cameras as external sensors and it closes the control loop by using image features. In recent years, different features have been proposed to have good performance in terms of accuracy for controlling parallel robots, for example the observation of robot legs [4] or the use of image moments [5].

Positioning accuracy is one of the most important criteria in the analysis of controller performance. For the case of external sensor-based control, the positioning accuracy depends on the error of observation of the features [6]. It has been proven in [6]

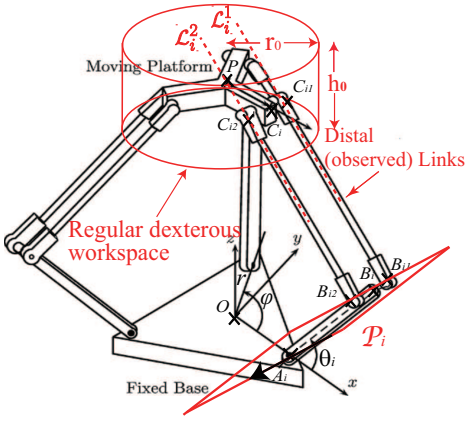

Fig. 1: DELTA robot mechanism

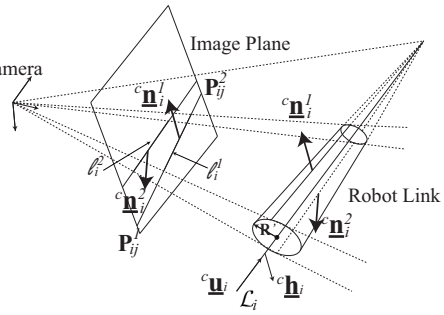

Fig. 2: Projection of a cylinder in the image

that controller properties such as the number and types of external sensors that are used, together with the kinds of features that are observed, can affect the observation error. Other factors that affect the positioning accuracy are the robot geometric parameters because they have impact on the interaction models, i.e. the models used to characterize the interaction between the observed object and the sensors, thus leading to effects on the positioning accuracy [7]. So taking the accuracy performance of controllers into account in robot design process is necessary. In this work, the accuracy performance of leg-based visual servoing and image moment visual servoing will be taken into account in the robot design process, so that we can get a DELTA robot for a given controller with the best accuracy performance. Compared to the previous work [8], this is the first time that control-based design approaches are applied to the optimal design of a spatial robot. Also this is the first time that image moment visual servoing is taken into account as one of the controllers in control-based design.

2 Robot Architecture and Specifications

The DELTA robot architecture is illustrated in Fig. 1. It is a parallel manipulator with three translational degrees of freedom (DOF). For the design of the robot, we fix the following specifications. The DELTA robot should cover a dexterous regular workspace [1] of cylindrical shape, its geometric size is given in Tab. 1. Some geometric and kinematic constraints should be satisfied throughout the regular workspace, such as: the robot should be free of singularity, the positioning accuracy should be lower than the requirements in given Tab. 1 [9]. For practical industrial reasons, the robot must be as compact as possible.

We decided to control the robot with visual servoing instead of usual model-based control in order to have better accuracy performance [3]. A single camera (2336 $\times$ 1728 pixels) of resolution and a focal length of 10 mm will be used in this case and the camera will be mounted onto the base platform.

Two types of standard visual servoing approaches will be applied to the control of a DELTA robot: leg-based visual servoing [4] and image moment visual servo-

Table 1: Requirements of the DELTA robot

Regular dexterous workspace size (radius of cylinder) r_0	$\geqslant$ 200 mm
Regular dexterous workspace size (height of cylinder) h_0	$\geqslant$ 100 mm
Positioning accuracy wherever in regular dexterous workspace	$\leqslant$ 0.5 mm

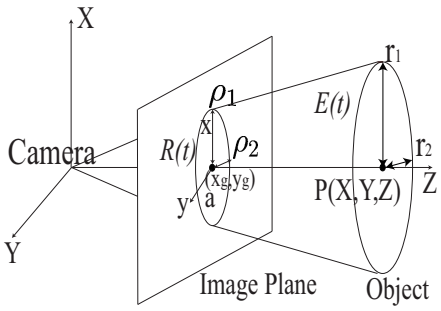

Fig. 3: Projection of an ellipse in the image plane

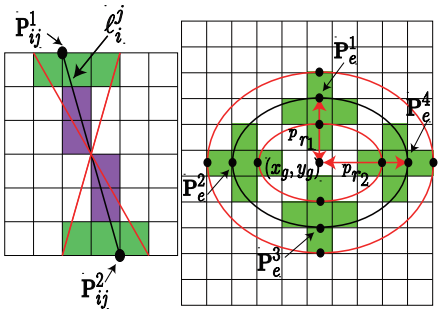

Fig. 4: One-pixel error on the intersection of the image boundary and the observed line [6] and one-pixel error on the top points of the ellipse

ing [5]. Leg-based visual servoing uses the features extracted from the observation of the DELTA robot distal links to do the control. The features are the unit vector $\underline{\mathbf{u}}_i$ of the line $\mathcal{L}_i$ passing through robot link cylinder axis or its Plücker coordinates $(\underline{\mathbf{u}}_i, \mathbf{h}_i)$ [4] (Fig. 2). Image moment visual servoing takes moments $\mathbf{m}$ of a visual target (here a circle or an ellipse, Fig. 3) projected in the image plane as the features to do the control [5]. For the DELTA robot, in this work, $\mathbf{m} = [x_g \ y_g \ a]^T$ where (x_g, y_g) are the coordinates of the center of the projected ellipse in the image plane, while a is its surface (Fig. 3). Once the visual features $\mathbf{s}$ ($\underline{\mathbf{u}}$,($\underline{\mathbf{u}}$ $\mathbf{h}$) or $\mathbf{m}$) are selected, we can always find the relationship between the time variation $\dot{\mathbf{s}}$ of $\mathbf{s}$ and the relative camera-object kinematics screw $\mathbf{v}$ by [5]

$$\dot{\mathbf{s}} = \mathbf{L}_s \mathbf{v} \tag{1}$$

Where $\mathbf{L}_s$ is the interaction matrix related to $\mathbf{s}$. For reasons of page limits, no recalls are provided on visual servoing. Interested readers should refer to ([3],[4],[5],[10]).

3 Controller-based Robot Performance

With respect to the accuracy requirements for the robot design, two types of controller performance will be considered. One is the positioning error of visual servoing, which comes from the camera observation capacities and the interaction model [5]. The other one is the controller singularities, i.e. the singularities of the interaction matrices, which impact both positioning accuracy and controller stability [3].

3.1 Positioning Error Models

Positioning error models for leg-based visual servoing For leg-based visual servoing control, the positioning error comes from the camera observation error of the leg directions or leg Plücker coordinates [6]. In this work, we decide to observe all the six legs of the DELTA robot since the observation redundancy helps get the best control accuracy.

In Figure 2, we see that the projections of a robot link in the image plane are two lines ℓ_i^1, ℓ_i^2. The intersection points of ℓ_i^j $(j = 1, 2)$ and the image plane boundary are denoted as $\mathbf{P}_{ij}^1, \mathbf{P}_{ij}^2$. Similarly as it was done in [8], we add a random shift in pixels on $\mathbf{P}_{ij}^1, \mathbf{P}_{ij}^2$ (Fig. 4) to model the noise we got from the observation. Based on [10], we can always find the relationship between the camera-object kinematic screw to the time derivative of $\mathbf{P}_{ij}^1, \mathbf{P}_{ij}^2$. Since the error of observation is very small, the first-order geometric models can be used and the error models relating the movement of end-effector $\boldsymbol{\delta}\mathbf{x}$ to the variation $\boldsymbol{\delta}\mathbf{P}$ of the intersection points can be written under the form:

$$\boldsymbol{\delta}\mathbf{x} = \mathbf{S_u}\boldsymbol{\delta}\mathbf{P} \quad \text{(in the case of a leg-direction-based controller)} \tag{2}$$

$$\boldsymbol{\delta}\mathbf{x} = \mathbf{S_{uh}}\boldsymbol{\delta}\mathbf{P} \quad \text{(in the case of a line-based controller)} \tag{3}$$

Where $\mathbf{S_u}$ and $\mathbf{S_{uh}}$ are the Jacobian matrices linking the variation of positions for the intersection points $\mathbf{P}$ to the kinematics screw of end-effector, when using leg-direction-based visual servoing and line-based visual servoing. They can be computed with the help of the controller interaction matrices (for more details, see [8]). In image plane, one pixel is the smallest addressable element, thus every component of vector $\boldsymbol{\delta}\mathbf{P}$ equals ± 1.

Positioning error model for image moment visual servoing Similarly as it was done in [5], the shape of the picture observed is chosen to be an ellipse (Fig. 3). The image moments $\mathbf{m} = [x_g \ y_g \ a]^T$ are defined in Section 2 (Fig. 3). To model the observation error of the center of gravity and the area of the object in the image plane, we add a noise which is a random shift in the pixels on the coordinates of object center of gravity and of the top points of major and minor axes of the ellipse (see Fig. 4). Then we have:

$$\boldsymbol{\delta}\mathbf{x} = \mathbf{L}_m^+\boldsymbol{\delta}\mathbf{m} \tag{4}$$

Where $\boldsymbol{\delta}\mathbf{x}$ is the movement of end-effector, $\mathbf{L}_m^+$ is the pseudo-inverse of the interaction matrix related to the features $\mathbf{m}$, $\boldsymbol{\delta}\mathbf{m} = [\delta x_g \ \delta y_g \ \delta a]^T$ with $\delta x_g = \pm 1$, $\delta y_g = \pm 1$ and $\delta a = \pi[(\rho_1 \pm 1)(\rho_2 \pm 1) - \rho_1\rho_2]$ (ρ_1, ρ_2 are radii of the major and minor axes of ellipse projected to image plane in pixel as is shown in Fig. 4).

3.2 Controller Singularities

The visual servoing controller singularity appears when the interaction matrix is rank deficient (see [11] for more details).

Singularities of leg-direction-based visual servoing applied to the control of the DELTA robot have been studied in [12] and [7]. In these papers, it is shown that a

controller singularity will appear when all planes $\mathcal{P}_i$ ($i = 1, 2, 3$) containing points A_i and B_i and the axis of the active revolute joint located at point A_i (Fig. 1) are parallel.

Singularities of the line-based visual servoing are different. As known from [1], singularities of kinematic models are also singularities of the pose estimation models. When observing the six lines $\mathcal{L}_{ij}$ passing through the links $B_{ij}C_{ij}$ ($i = 1, 2, 3$, $j = 1, 2$, Fig. 1) of the DELTA robot in order to rebuild its end-effector pose, the robot platform orientation being always constant, the pose estimation model is equivalent to finding the common intersection point of the six lines $\mathcal{L}'_{ij}$ obtained from lines $\mathcal{L}_{ij}$ by a translation of vectors $\overrightarrow{C_{ij}P}$. The only condition of degeneracy of this pose estimation model is when all lines $\mathcal{L}'_{ij}$ are parallel, which means that the controller singularity of line-based visual servoing for the DELTA robot will appear when all its distal links are parallel.

For the singularity of image moment visual servoing, from [5], we see that the interaction matrix $\mathbf{L}_m$ is an upper triangular matrix. It can be singular if and only if the depth between the camera and the object is infinite which can never be reached or the projected area of the observed object in image plane equals zero which also means that the object is at infinity and it will never happen. Thus, these singularity cases will never happen in the image moment visual servoing of the DELTA robot.

4 Optimal Design Process

We assume that all the three chains of DELTA robot are identical in length, then the DELTA robot can be defined by the following geometric parameters: L_1, L_2, L_3, r_a, r_b, (in Fig. 5, $L_1 = L_{A_iB_i}$, $L_2 = L_{B_iC_i}$, $L_3 = L_{B_{i1}B_{i2}} = L_{C_{i1}C_{i2}}$, $r_a = L_{OA_i}$, $r_b = L_{PC_i}$). When leg-based visual servoing is applied, the radius R' of the cylindrical distal links of robot also affects the positioning error (Fig.2) [6]. (x_c, y_c, z_c) define the position of the camera with respect to the robot frame. The camera image plane is set to be parallel to the end-effector of the DELTA robot, and the coordinates (x_c, y_c) of the camera frame origin are set at $(0, 0)$ to observe all robot legs in a symmetrical way. r_1 and r_2 are the radii (in world frame) defining the ellipse in image moment visual servoing (Fig. 3). The method of getting the regular dexterous workspace is introduced in [9] and following performances must be satisfied throughout the dexterous workspace:

- Type 2 and constraint singularity-free: ensuring the DELTA robot will not meet any Type 2 or constraint singularities.
- controller singularity-free: no singularities of the controllers
- end-effector in image: ensuring that all the robot distal legs can be observed when using leg-based visual servoing, as well as the ellipse shape picture on the end-effector when using image moment visual servoing.
- required positioning accuracy: Maximal positioning error computed with the models of Section 3 should be lower than 0.5 mm.
- no link collision in the workspace.

Since the three chains of DELTA robot are identical in length, we study the bounding box of a single chain of the DELTA robot in order to study its footprint. This bounding box is shown in Fig. 5. The objective function amounts to the volume $V = S \cdot L_3$ of the bounding box in Fig. 5 when the link A_iB_i and B_iC_i are perpendicular, where S is

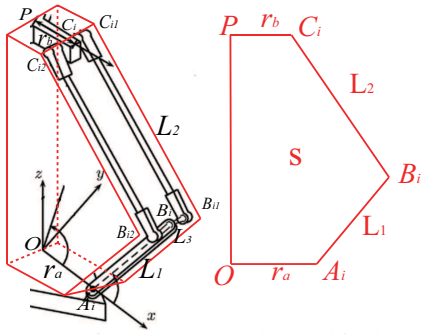

Fig. 5: Bounding box of DELTA robot leg and its home configuration

Table 2: Design parameters and value of the objective function as a function of the chosen controller

	Line-based visual servoing (observe 6 legs)	Leg-direction-based visual servoing (observe 6 legs)	Image moment visual servoing
r_a[m]	0.1741	0.2213	0.1292
r_b[m]	0.0530	0.0631	0.0513
L_1[m]	0.5614	0.6680	0.5844
L_2[m]	0.3060	0.4668	0.3742
L_3[m]	0.0856	0.1066	0.0852
z_c[m]	0.0500	0.0500	0.1289
R'[m]	0.015	0.020	N/A
r_1[m]	N/A	N/A	0.0254
r_2[m]	N/A	N/A	0.0254
V[m^3]	0.01345	0.02873	0.01461

the lateral surface of the box. In order to create a compact DELTA robot which has the specifications detailed in Tab. 1, the following optimization problem is formulated:

$$\begin{aligned} \text{minimize} \quad & V = S \cdot L_3 \quad (S = ((r_a + r_b) \cdot \sqrt{L_1^2 + L_2^2 - (r_a - r_b)^2} + L_1 \cdot L_2)/2) \\ \text{over} \quad & \mathbf{x} = [r_a \ r_b \ L_1 \ L_2 \ L_3 \ z_c \ R'] \\ & \text{(leg-direction-based and line-based visual servoing)} \\ & \mathbf{x} = [r_a \ r_b \ L_1 \ L_2 \ L_3 \ z_c \ r_1 \ r_2] \text{ (image moment visual servoing)} \\ \text{subject to} \quad & r_0 \geqslant 200 \text{ mm}, \ h_0 \geqslant 100 \text{ mm} \end{aligned} \tag{5}$$

Where: r_0 is the radius of the cylindrical dexterous workspace of the DELTA robot and h_0 is its height. The algorithm of computing the size of the maximal dexterous workspace is presented in [9].

The previous optimization algorithm is applied for the design of the mentioned DELTA robot and the optimal design results are given in Tab. 2. We see from the Tab. 2 that the robot size (volume of the bounding box V) designed for image moment visual

Table 3: Positioning errors for the three robot designs

Desired point coordinate [m]	Leg-direction-based [m]	Line-based [m]	Image moment [m]
(0.2,0,-0.05)	4.17e-4	3.61e-4	2.28e-4
(0.2,0,0)	4.92e-4	3.79e-4	2.49e-4
(0.2,0,0.05)	5.63e-4	4.31e-4	2.53e-4
(0.17,0.1,-0.05)	4.73e-4	4.63e-4	2.34e-4
(0.14,0.14,-0.05)	4.14e-4	4.42e-4	2.00e-4
(0.14,0.14,0.05)	4.86e-4	5.58e-4	2.66e-4

servoing is almost the same as for the robot size designed for line-based visual servoing. When using leg-direction-based visual servoing, the robot size is twice the size of the robot designed for the other two controllers.

5 Simulation and Result Analysis

In order to verify the results we got from the optimization, simulations are performed in a connected ADAMS-Simulink environment. We created three DELTA robot mechanical models in ADAMS using the results got from the optimal design (one model per controller). Their controllers were developed with Matlab/Simulink. Similarly as it was developed in [13], we simulated a measurement noise of one pixel for the observation (see Fig. 4), so that controller accuracy performance can be checked. In all these simulations, we set a home position and several desired positions within the dexterous workspace. Then DELTA robots performed motions from their home position to the desired positions and we checked their positioning errors.

All the simulation results are shown in the Tab 3. Desired points coordinates are with respect to the cylindrical regular workspace base frame whose origin is the center of the cylindrical workspace.

From these simulation results, even if the error models defined in Section 3 were simplified, resulting optimized robots have a maximal accuracy of around 0.5 mm for all points tested in their workspace. Leg-direction-based visual servoing leads to the poorest positioning accuracy. Additionally, when using image moments, the controller accuracy is better than line-based controller. However the difference of accuracy between image moment visual servoing and line-based visual servoing is not significant.

6 Conclusion

In this paper, we performed "control-based design" of a DELTA robot in order to obtain the best accuracy performance of the robot with its controller. We optimized the design of DELTA robot for three different types of controllers: leg-direction-based visual servoing, line-based visual servoing and image moment visual servoing. Based on these three controllers, we developed positioning error models taking into account the error of observation coming from the camera. We also analyzed the singularities of these controllers to be sure that no singularity of the controller appeared in the final design of the

robot, thus avoiding instability issues. Then, design optimization problems have been formulated in order to find the optimal geometric parameters and camera placement for the DELTA robot for each type of controller. The simulation results showed that the robot designed for image moment visual servoing was more compact and had better accuracy performance than the other two robots optimized for other control techniques. However the differences of robot size and accuracy between the image moments controller and line-based controller were not significant enough in order to draw general conclusions. Therefore, experimental works on real prototypes should be done in the next step in order to verify the simulation results.

Acknowledgements

This work has been partially funded by the French ANR project SESAME (funding ID: ANR-18-CE33-0011).

References

1. Merlet, J.-P., 2006. Parallel robots, Vol. 128. Springer Science & Business Media.
2. Merlet, J.-P., 2012. http://www-sop.inria.fr/members/Jean-Pierre.Merlet/merlet.html.
3. Chaumette, F., Hutchinson, S., and Corke, P., 2016. "Visual servoing". In Springer Handbook of Robotics. Springer, pp. 841–866.
4. Andreff, N., Dallej, T., and Martinet, P., 2007. "Image-based visual servoing of a gough-stewart parallel manipulator using leg observations". The International Journal of Robotics Research, **26**(7), pp. 677–687.
5. Tahri, O., and Chaumette, F., 2005. "Point-based and region-based image moments for visual servoing of planar objects". IEEE Transactions on Robotics, **21**(6), pp. 1116–1127.
6. Kaci, L., Boudaud, C., Briot, S., and Martinet, P., 2018. "Elastostatic modelling of a wooden parallel robot". In Computational Kinematics. Springer, pp. 53–61.
7. Briot, S., Rosenzveig, V., Martinet, P., Özgür, E., and Bouton, N., 2016. "Minimal representation for the control of parallel robots via leg observation considering a hidden robot model". Mechanism and Machine Theory, **106**, pp. 115–147.
8. Kaci, L., Briot, S., Boudaud, C., and Martinet, P., 2017. "Control-based design of a five-bar mechanism". In New Trends in Mechanism and Machine Science. Springer, pp. 303–311.
9. Germain, C., Caro, S., Briot, S., and Wenger, P., 2013. "Optimal design of the irsbot-2 based on an optimized test trajectory". In ASME International Design Engineering Technical Conferences & Computers and Information in Engineering Conference IDETC/CIE 2013.
10. Andreff, N., Espiau, B., and Horaud, R., 2002. "Visual servoing from lines". The International Journal of Robotics Research, **21**(8), pp. 679–699.
11. Hutchinson, S., Hager, G. D., and Corke, P. I., 1996. "A tutorial on visual servo control". IEEE Transactions on Robotics and Automation, **12**(5), pp. 651–670.
12. Rosenzveig, V., Briot, S., and Martinet, P., 2013. "Minimal representation for the control of the adept quattro with rigid platform via leg observation considering a hidden robot model". In 2013 IEEE/RSJ International Conference on Intelligent Robots and Systems.
13. Vignolo, A., Briot, S., Martinet, P., and Chen, C., 2014. "Comparative analysis of two types of leg-observation-based visual servoing approaches for the control of the five-bar mechanism". In Proceedings of the 2014 Australasian Conference on Robotics and Automation (ACRA 2014). University of Melbourne, Australia.